Photopolymerization of Two-Component Monolayers: Mixtures of Bis[2-(*n*-hexadecanoyloxy)ethyl]methyl(4-vinylbenzyl)ammonium Chloride and Dioctadecyldimethylammonium Bromide

S. Q. Xu[1] and J. H. Fendler*

Department of Chemistry, Syracuse University, Syracuse, New York 13244-1200.
Received August 8, 1988; Revised Manuscript Received December 15, 1988

ABSTRACT: Monolayers, on aqueous 5.0×10^{-3} M NaCl, have been prepared from mixtures of bis[2-(*n*-hexadecanoyloxy)ethyl]methyl(4-vinylbenzyl)ammonium chloride (**1**) and dioctadecyldimethylammonium bromide (**5**). Surface area–surface pressure isotherms, determined for 0, 0.2, 0.4, 0.6, 0.8, and 1.0 mole fractions of **1** (x_1) in **1** + **5**, led to collapse pressures (Π_c) of 53, 57, 60, 69, 69, and 67 mN m^{-1} and to collapse areas (ω_c) of 51, 48, 45, 42, 38, and 32 Å^2 per molecule, respectively. The obtained two-dimensional Π_c–x_1 phase diagram, plateauing at $x_1 \approx 0.6$, indicated the complete but nonideal miscibility of **1** and **5** and the pressure of a surface azeotrope. Thermodynamic treatment of the data allowed the calculation of the collapse pressures and the compositions of the collapse phase. Treatment of ω_c values as a function of x_1 led to a value of 1.3 kJ mol^{-1} for the excess free energy of interaction of **1** and **5** in the monolayers. This value is more positive than that given for the free energy of ideal mixing (−1.7 kJ mol^{-1}), indicating the fulfillment of the thermodynamic requirement for mixing. Ultraviolet irradiation of monolayers prepared from mixtures of **1** and **5** resulted in the photopolymerization of **1** in the matrix of the mixed monolayer. Photopolymerization rates (expressed as decay times for the depletion of monomeric **1**, τ values) have been determined as a function of x_1, surface pressure, and irradiation intensity. τ values were found to increase with a decreasing mole fraction of **1**. Kinetics of photopolymerization have been treated in terms of a two-dimensional patch polymerization model and in terms of a classical photoinitiation, propagation, and termination model. These treatments led to the assessment of the average degrees of photopolymerization, $\bar{L}$ value. Decreasing the intensity of irradiation or increasing x_1 increased the $\bar{L}$ values.

Introduction

The inherent interest in two-dimensional reactivities and potential applicability have prompted the renaissance of molecular monolayers and organized multilayers (Langmuir–Blodgett (LB) films) as an area of vigorous research activity.[2-5] Applications in molecular electronic and sensing devices require a high degree of uniformity, controllable morphology, and long-term system stability. Polymerization of monolayers and LB films has provided an approach toward meeting these requirements. Surfactants and lipids containing diacetylene, vinyl, acryl, methacryl, and styryl moieties have been polymerized as monolayers at air–water interfaces and as LB films on a variety of substrates.[6-15]

Following our interest in polymerized vesicles and bilayer (black) lipid membranes,[16-22] we have launched complementary and systematic studies in monolayers and LB films. Initially, we reported results on the photopolymerization of monolayers prepared from bis[2-(*n*-hexadecanoyloxy)ethyl]methyl(4-vinylbenzyl)ammonium chloride (**1**, Chart I), di-*n*-octadecylmethyl(*p*-vinylbenzyl)ammonium chloride (**2**), dioctadecylmethyl[2-[[(4-vinylphenyl)oxy]carbonyl]ethyl]ammonium chloride (**3**), and *n*-hexadecyl [11-(4-vinylbenzamido)undecyl]phosphate (**4**).[23] Polymerization was found to decrease the molecular area of monolayers prepared from **1** and **2**, have no effect on that formed from **3**, and increase that prepared from **4**. Rate constants for the photopolymerization of monolayers prepared from **1** have been elucidated at different surface pressures and irradiation energies. Treatment of the kinetic data, in terms of either a classical or a two-dimensional patch polymerization model,[18] led to the assessment of the average degrees of polymerization ($\bar{L}$ values). $\bar{L}$ values were found to be profoundly influenced by the intensity of the irradiation. At low intensity, they reached values in the hundredths. However, they ranged between 11 and 27 at higher intensities.[22] In contrast, the average degree of photopolymerization of vesicles prepared from **1**, even at comparably low irradiation levels, was found to be on the order of 2–20.[18] The looser surfactant packing in the vesicles than that in monolayers was suggested to be responsible for the different degrees of photopolymerization.[20]

The characterization and polymerization of monolayers prepared from mixtures of **1** and dioctadecyldimethylammonium bromide (**5**) are the subjects of the present report. Collapse pressures and collapse areas, obtained from surface pressure–surface area isotherms, have been analyzed thermodynamically as functions of the monolayer composition. Similarly, rate constants and degrees of photopolymerization have been determined as functions of the mole fraction of **1** in monolayers prepared from mixtures of **1** and **5**.

Experimental Section

Preparation, purification, and characterization of the surfactants **1**–**5** have been described.[22] HPLC-grade chloroform (Aldrich) was used as received. Reagent grade NaCl was baked at 800 °C for several hours prior to making up solutions for the subphase. Water was purified by a Millipore Milli-Q filter system provided with a 0.22-μm Millistack filter at the outlet. The specific resistivity of the water used was 18 MΩ cm at 25 °C. Nitrogen was high-purity dry grade (Union Carbide).

A commercial Lauda Model P film balance was used for surface pressure–surface area isotherm determinations. Operation of the film balance was controlled by a Zenith Data System. The surface pressure–surface area isotherms were visualized on the CRT screen, and data were plotted by a Hewlett-Packard *x*–*y* recorder. The area and pressure sensitivities were 0.2 Å^2/molecule and 0.1 mN/m, respectively. Surface pressure was calibrated by applying the calibration weight onto the calibration cross. The maximum area available for spreading was 583 cm^2.

Spreading solutions were prepared by dissolving the surfactants in HPLC-grade chloroform just prior to spreading. Spreading solution (100 μL, 4×10^{17} molecules/mL) was spread on the surface of 5.0 mM NaCl solution, giving an initial molecular area of 145.8 Å^2/molecule at $\pi = 0$. Nitrogen atmosphere was maintained in the trough during spreading, solvent evaporation, and measurements. The surface of the subphase was cleared several

0024-9297/89/2222-2962$01.50/0

Chart I

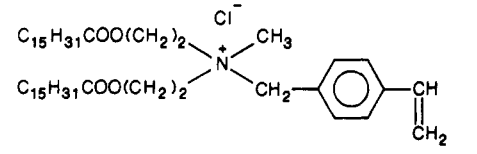

1

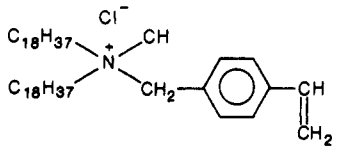

2

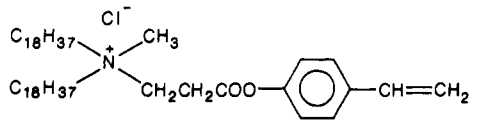

3

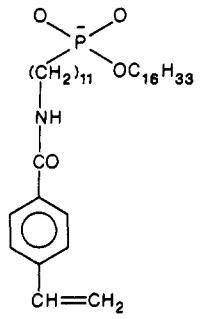

4

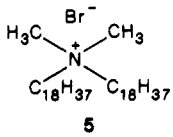

5

times prior to monolayer formation by sweeping with a Teflon barrier or by aspiration. The subphase was deemed clean when the surface pressure increase was less than 0.2 mN m^{-1} upon compression to one-twentieth of the original area and when this pressure increase remained the same subsequent to aging for several hours (criteria of minimal aging of the surface).[24] Effect of solvent was checked by injecting 200 μL, of $CHCl_3$ on the surface and compressing it to the minimum area available. No visible residual effect could be observed.

Monolayers, formed from different mixtures of 1 and 5, were polymerized in a nitrogen atmosphere by irradiation by a 4-W UV lamp placed 2 cm above the surface of the monolayer. The intensity of irradiation was attenuated by placing filters into the beam path. The lamp intensity (without any alteration) was determined to be 10 ± 2 μW/cm^2 at 250 ± 3 nm by a Model 2232 optical power meter. Polymerizations were followed by monitoring monolayer area variations with time at a constant pressure on the Hewlett-Packard x–y recorder.

Results and Discussion

Surface Pressure–Surface Area Isotherms. Surface pressure–surface area isotherms of monolayers prepared from 1 and 5 and from their mixtures (0.2, 0.5, 0.6, and 0.8 mole fraction of 1 in 1 + 5) on 5.0 mM aqueous NaCl are shown in Figure 1. All isotherms show the expected behavior. At low surface pressure, lying on the subphase, molecules occupy large areas. With increasing surface pressures they begin to be squeezed and orient their hydrophobic tails away from the surface. Following a partially and more fully condensed state, there is a transition to a compressed (solid) state in the region of 20–36 mN m^{-1}. This transition is characterized by a pressure, Π_i, and

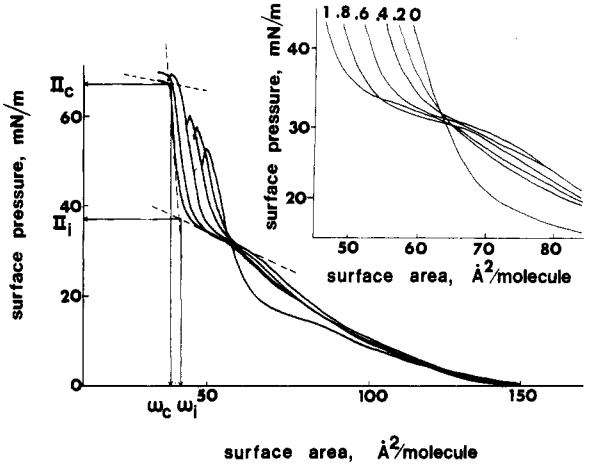

Figure 1. Surface area–surface pressure isotherms for spreading 1, 5, and mixtures of 1 + 5 at 0.2, 0.4, 0.6, and 0.8 mole fractions of 1 on aqueous 5.0 mM NaCl. Areas (ω_i) and pressures (Π_i) associated with the transition to a compressed state were taken by projecting the intersection of straight lines drawn to the appropriate sections of the isotherm to the surface area and surface pressure axes. The collapse pressure (Π_c) and collapse area (ω_c) were taken by treating that transition, similarly. The insert shows an expansion of the isotherms between 20 and 40 mN/m. Temperature = 24.0 ± 0.5 °C.

Table I
Surface Pressure–Surface Area Isotherms[a]

mol fract of 1 in 1 + 5	ω_i, Å²	ω_c, Å²	Π_c, mN/m	Π_i, mN/m
0[b]	61	51	53	20
0.2	50	48	57	35
0.4	49	45	60	34
0.6	46	42	69	35
0.8	45	38	69	35
1.0[b]	42	38	67	36

I = 3.15[c]

$\Delta\epsilon$ = 1.3 kJ/mol[d]

[a] See the Experimental Section for description of spreading conditions. Temperature = 24.0 ± 0.5 °C, 5.0 × 10^{-3} M NaCl as subphase. Compression speed = (1–5) × 10^{-3} Å²/(molecule s). See Figure 1 for definitions of ω_i, ω_c, Π_i, and Π_c. [b] Taken from ref 23. [c] Calculated by eq 11. [d] Calculated by eq 4.

by a corresponding area, ω_i. It is interesting to observe that all isotherms intersect in the vicinity of 30 mN m^{-1} and that the surface pressure–surface area isotherms above this pressure are arranged according to their composition (see insert in Figure 1). The equation of state of the "solid" monolayer is characterized by a relatively small change in the surface area with increasing surface pressure. This state prevails until the collapse of the monolayer, characterized by the collapse pressure, Π_c, and collapse area, ω_c. The method of taking ω_c, ω_i, Π_c, and Π_i from the isotherms is illustrated in Figure 1, and the values obtained are collected in Table I.

Effect of Monolayer Composition on Collapse Pressure. The collapse pressure of the monolayer prepared from 5 (53 mN m^{-1}) is 14 mN m^{-1} smaller than that prepared from 1. Increasing the mole fraction of 1 (x_1), in monolayers prepared from mixtures of 1 and 5 resulted in increased collapse pressures up to a plateau of Π_c = 69 mN m^{-1} between x_1 = 0.6 and x_1 = 0.8. After this plateau, Π_c decreased to 67 mN m^{-1} at x_1 = 1 (Figure 2).

Insoluble monolayers, prepared from a mixture of two surfactants, can be treated in terms of surface pressure (Π)–composition (x) two-dimensional phase diagrams if the external pressure (P) and temperature (T) are kept constant.[25-32] The collapse pressure of a monolayer con-

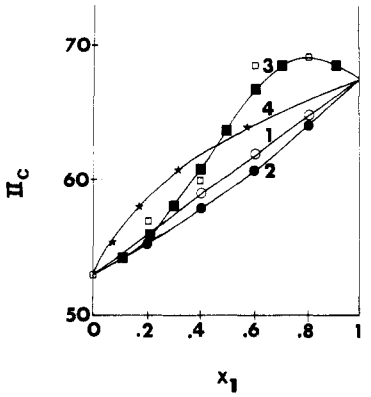

Figure 2. Plot of the experimentally determined collapse pressures (Π_c values) against x, the mole fraction of 1 in 1 + 5 (□). Also shown are the values calculated for ideal behavior by using eq 6 (line 1) and those by using eq 7 (line 2), 9 (line 3), and 10 (line 4).

taining two components (1 and 5) that are completely miscible is given by[29-31]

$$x_1^{M} f_1 \exp\left(\frac{\Pi_{c,m} - \Pi_{c,1}}{\kappa T}\omega_1\right) + x_5^{M} f_5 \exp\left(\frac{\Pi_{c,m} - \Pi_{c,5}}{\kappa T}\omega_5\right) = 1 \quad (1)$$

where x_1^{M} and x_5^{M} are the mole fraction in the monolayer (indicated by the superscript M) of surfactants 1 and 5, respectively; $\Pi_{c,1}$, $\Pi_{c,5}$, and $\Pi_{c,m}$ are monolayer collapse pressures of pure 1, pure 5, and those of mixtures of 1 and 5 at a given composition (x_1^{M}, x_5^{M}), respectively; ω_1 and ω_5 are limiting surface areas (ω_c values in Table I) at the collapse point; f_1 and f_5 are surface activity coefficients at the collapse point of components 1 and 5, respectively; and κ and T are Boltzman's constant and the absolute temperature.

The activity coefficients are related to x_1^{M} and x_5^{M} by the interaction parameter I

$$f_1 = \exp[I(x_5^{M})^2] \quad (2)$$

$$f_5 = \exp[I(x_1^{M})^2] \quad (3)$$

and hence to the interaction energy, $\Delta\epsilon$:

$$\Delta\epsilon = I\kappa T/6 \quad (4)$$

Substitution of eq 2 and 3 into eq 1 leads to

$$x_1^{M} \exp\left(\frac{\Pi_{c,m} - \Pi_{c,1}}{\kappa T}\omega_1\right) \exp[I(x_5^{M})^2] + x_5^{M} \exp\left(\frac{\Pi_{c,m} - \Pi_{c,5}}{\kappa T}\omega_5\right) \exp[I(x_1^{M})^2] = 1 \quad (5)$$

In the absence of interactions, $f_1 = 1$, $f_5 = 1$, and

$$\Pi_{c,m} = x_1^{M}\Pi_{c,1} + x_5^{M}\Pi_{c,5} \quad (6)$$

Changes in the collapse pressure of monolayers prepared from mixtures of 1 and 5 as a function of x_1^{M} will, therefore, be ideal (see line 1 in Figure 2). In the presence of interactions, $\Pi_{c,m}$ will deviate, of course, from ideal behavior. Expansion of eq 1 (or 5) and neglect of the higher order terms lead to

$$\Pi_{c,m} = \frac{x_1^{M}\omega_1\Pi_{c,1} + x_5^{M}\omega_5\Pi_{c,5}}{x_1^{M}\omega_1 + x_5^{M}\omega_5} \quad (7)$$

which allows the approximation of $\Pi_{c,m}$ values of different composition of surfactants. Line 2 in Figure 2 was calculated by substituting the appropriate parameters (given in Table I) into eq 7.

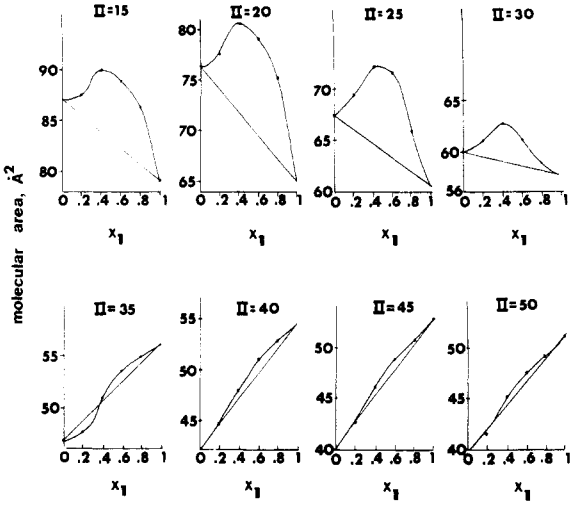

Figure 3. Plots of molecular areas as functions of the mole fraction of 1 in 1 + 5 at different surface pressures (Π in mN/m).

A maximum value in the collapse pressure at a given composition (Figure 2) is indicative of a surface azeotrope,[29-31] characterized by

$$(\partial\Pi_{c,m}/\partial x_i^{M})_{P,T} = 0 \quad (8)$$

and the interaction parameter at the "azeotrope" is given by:[30]

$$I = \left[\frac{-(\Pi_{c,1} - \Pi_{c,m})}{\kappa T(x_5^{M})^2}\omega_1\right]_{P,T} = \left[\frac{-(\Pi_{c,5} - \Pi_{c,m})}{\kappa T(x_1^{M})^2}\omega_5\right]_{P,T} \quad (9)$$

Using eq 9 allowed the assessment of the interaction parameter to be +3.15, which, in turn (by eq 4), led to the a value of 1.3 kJ/mol for the interaction energy between 1 and 5. Line 3 in Figure 2 has been drawn according to eq 5 and 9.

The relationship between the collapse pressure $\Pi_{c,m}$ and composition of the collapse phase (x_1^{B} and x_5^{B}) at the point of collapse is also shown in Figure 2 (line 4). Values have been evaluated by

$$x_1^{B} = a_1 x_1^{M} \exp\left(\frac{\Pi_{c,m}\omega_1}{\kappa T}\right) \quad (10)$$

where a_1 was determined from

$$a_1 = \exp\left(-\frac{\Pi_{c,1}\omega_1}{\kappa T}\right) \quad (11)$$

Effect of Monolayer Composition on Collapse Area. Excess Free Energy of Interaction. Molecular area changes as a function of the monolayer composition at a given constant pressure are shown in Figure 3. Pronounced positive deviations are evident in the 15–30 mN m^{-1} pressure range. At higher pressures transition occurs (Figure 1) and the behavior of the monolayer becomes more ideal with respect to the surface areas occupied by its constituents.

Evaluation of the excess free energy of interaction at a given surface pressure, ΔG_{xs}, provides a more quantitative description of the mixing of the surfactants in the monolayer.[25,26,33-36] As was shown, 1 and 5 are miscible and behave ideally in the limit of zero pressure; then

$$\Delta G_{xs} = \int_0^{\Pi} (\omega_{1,5} - x_1^{M}\omega_1 - x_5^{M}\omega_5)\, d\Pi \quad (12)$$

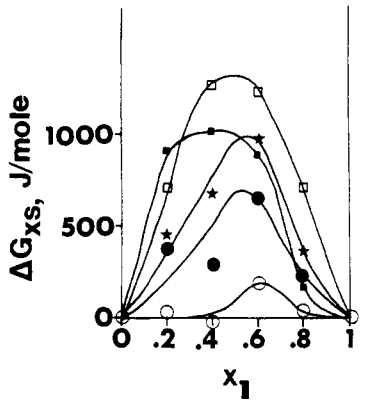

Figure 4. Plots of ΔG_{xs}^{Π} vs mole fraction of 1 in 1 + 5 at 50 (□), 40 (■), 30 (★), 20 (●), and 10 (○) mN/m.

where ω_1^{Π}, ω_5^{Π}, and $\omega_{1,5}^{\Pi}$ are the areas per molecule at pressure Π for pure components 1 and 5 and for the mixture, respectively. The integration has been carried out for five different surface pressures, and the results are shown in Figure 4. Excess free energies are seen to deviate progressively from ideality as the surface pressure increases from 10 to 50 mN m^{-1}. Maximum deviation occurs, as in many other mixed monolayers,[34-36] in the 0.5 mole fraction region. ΔG_{xs}^{Π} was calculated to be 1.3 kJ mol^{-1} at a surface pressure of 50 mN/m.

Negative free energy of mixing is a thermodynamic requirement for miscibility of 1 and 5 in the monolayer. This free energy mixing, ΔG_{mix}, is given by

$$\Delta G_{mix} = \Delta G_{xs}^{\Pi} + \Delta G_{id} \leq 0 \quad (13)$$

where ΔG_{id}, the free energy for ideal mixing at 1:1 mole ratio, is given by

$$\Delta G_{id} = RT(x_1^M \ln x_1^M + x_5^M \ln x_5^M) = -1.7 \text{ kJ mol}^{-1} \quad (14)$$

Substituting values for ΔG_{xs}^{Π} (1.3 kJ mol^{-1}) and ΔG_{id} (−1.7 kJ mol^{-1}) into eq 13 leads to negative ΔG, and thus the thermodynamic requirement of miscibility is fulfilled.

Thermodynamic analysis of surface pressure and surface area isotherms revealed the nonideal miscibility of nonpolymerizable **5** and polymerizable **1** surfactants in monolayers. Maximum collapse pressure of the monolayer was reached sharply at a mole fraction of 0.6 in mixtures of 1 and **5**.

Photopolymerization of Monolayers Prepared from Mixtures 1 and 5. Kinetics of photopolymerization of monolayers prepared from mixtures of 1 and **5** were followed at different surface pressures and at different light intensities by monitoring the changes of surface areas as functions of irradiation time. Irradiations have not led to photocleavage.[37] Typical traces of surface area changes accompanying photopolymerizations are illustrated in the insert in Figure 5.

Stopping the irradiation prior to the photopolymerization interrupted the surface area change. Upon the restart of irradiation, the area of the monolayer continued to decrease at the same rate as it had previously.

Surface area changes of monolayers upon photopolymerization have been shown to be best accommodated in terms of 15,[23] where ω_t, ω_∞, and ω_0 are surface areas of

$$\frac{\omega_t - \omega_\infty}{\omega_0} = \frac{\omega_0 - \omega_\infty}{\omega_0} e^{-t/\tau} \quad (15)$$

the monolayer at time t, subsequent to, and prior to polymerization, respectively, and τ is the decay time for the depletion of monomeric 1. Equation 15 fitted the experimental data obtained for the photopolymerization of

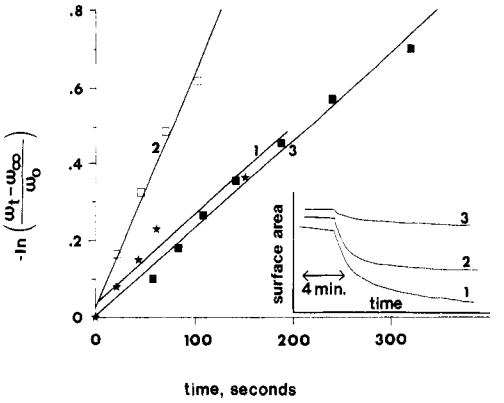

Figure 5. Inset: Changes of molecular areas at constant surface pressures of 21 (1), 30 (2), and 40 (3) mN m^{-1} as a function of irradiation time for monolayers prepared from mixtures of 1 and 5 (x_1 = 0.8). In the figure, the same data are plotted according to eq 15.

Table II
Kinetics of Photopolymerization of Monolayers Prepared from Mixtures of 1 and 5[a]

mol fract of 1 in 1 + 5	surf. press., mN m^{-1}	irradiation int[b]	τ, s	$\bar{L}$[c]	τ_{av},[d] s	k_p/k_t[d]
0.2	21	3.0×10^{-4}	711	44		
	30	3.0×10^{-4}	6184	5.1		
	40	3.0×10^{-4}	6595	4.8		
0.4	21	3.0×10^{-4}	643	49		
	30	3.0×10^{-4}	490	64		
	40	3.0×10^{-4}	1333	24		
0.6	21	3.0×10^{-4}	383	82	57	0.25
	21	1.1×10^{-4}	513	167	50	0.26
	21	2.7×10^{-5}	1149	304	99	0.29
	21	9.9×10^{-6}	1222	780	88	0.27
	30	3.0×10^{-4}	303	104		
	40	3.0×10^{-4}	835	38		
	40	1.1×10^{-4}	1469	58		
	40	2.7×10^{-5}	2155	162		
	40	9.9×10^{-6}	6765	141		
0.8	21	3.0×10^{-4}	400	79		
	30	3.0×10^{-4}	225	140		
	40	3.0×10^{-4}	456	69		
1.0[e]	11	3.0×10^{-4}	163	193	89	2.9
	21	3.0×10^{-4}	205	153	244	7.6
	26	3.0×10^{-4}	145	217		
	26	1.1×10^{-4}	333	258		
	26	2.7×10^{-5}	556	628		
	26	9.9×10^{-6}	595	1602		
	36	3.0×10^{-4}	94	335	182	12.2
	40	3.0×10^{-4}	137			
	45	3.0×10^{-4}	135	233	397	14.5

[a] Temperature = 24.0 ± 0.5 °C, 5.0 × 10^{-3} M NaCl as subphase. [b] Expressed as $\bar{\epsilon}\bar{I}$, see text and note 39 for details. [c] Determined by eq 35. [d] Determined by eq 49. [e] Taken from ref 23.

monolayers prepared from mixtures of 1 and **5** (Figure 5) reasonably well. Upward curvatures were observed, however, in some of the kinetic plots. This observation was entirely consistent with the proposed two-dimensional patch-type photopolymerization model.[18] Alternatively, upward curvatures in the kinetic data may be the consequence of the uncertainties in the infinity values used. These uncertainties may, in turn, originate in the monolayer dissolution, slow collapse during and subsequent to the polymerization, and cause spurious mechanical effects. It is preferred, as it was previously,[23] to present the data in terms of single pseudo-first-order lifetimes (obtained from plots similar to those shown in Figure 5) whose linearity extend to at least 2 half-lives of photopolymerization.

Photopolymerization decay times increase with decreasing mole fraction of 1 in the monolayers prepared

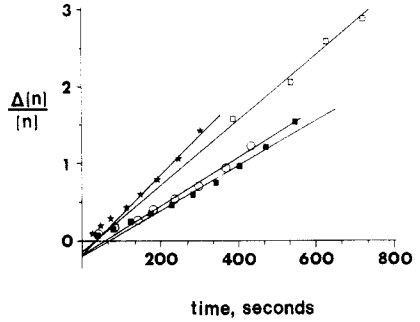

Figure 6. Plots of $\Delta[n]/[n]$ against time (eq 49) for the photopolymerization of monolayers prepared from 1 + 5 ($x_1 = 0.6$) at 21 mN m^{-1} by using irradiations of $\bar{\epsilon}\bar{I} = 3.0 \times 10^{-4}$ (□), 1.1×10^{-4} (★), 2.7×10^{-5} (■), and 9.9×10^{-6} (○).

from mixtures of 1 and 5 (Table II). The two-dimensional patch-type polymerization model predicts, in fact, this behavior.[18] This model assumes the propagation of the photogenerated radical chain in two-dimensional patches. Once a free radical (R•) forms from 1 it will most likely "chain" to its nearest neighbor. Hence, the effective concentration of monomeric 1 that R• sees is determined by the distribution of 1 in its neighborhood. As a first approximation, hexagonal packing of surfactants in the monolayers could be considered. At a low mole fraction of 1, the number of polymerizable monomers (moles of 1) available for R• is limited. Chain propagation requires, therefore, more extensive lateral mobility and longer lived propagating radicals. This will manifest in increased polymerization or lifetimes. At low mole fractions of 1, τ values are also increased with increasing surface pressures (Table II).

Kinetics of monolayer photopolymerizations have been analyzed in terms of two models:[23] the two-dimensional patch polymerization model (PPM), already alluded to and the classical approach (CPM) which considers photoinitiation, propagation, and termination rates.

The PPM model describes the photopolymerization of monolayers prepared from mixtures of 1 and 5 by equations 16–20,[38]

$$M \xrightarrow{h\nu} R_1 \tag{16}$$

$$R_1 + M \xrightarrow{k_p} R_2 \tag{17a}$$

$$R_2 + M \xrightarrow{k_p} R_3 \tag{17b}$$

$$R_{n-1} + M \xrightarrow{k_p} R_n \tag{17c}$$

where M is the free monomer, R is the propagating radical, and R_n is made up of a chain of $n-1$ monomers added to R_1. The set of reactions described by eq 17 constitutes the chain propagation. The same rate constant k_p is written for each propagation step, assuming that the radical reactivity is independent of the chain length. The propagation of the radicals is terminated by

$$R_m + R_n \xrightarrow{k_t} P_{m+n} \tag{18}$$

$$R_m + R_n \xrightarrow{k_t} P_m + P_n \tag{19}$$

where P_m, P_n, and P_{m+n} represent polymer molecules having the number of units indicated by their subscripts. Reactions 18 and 19 describe combination (coupling) and disproportionation, respectively. Since both of these reactions are bimolecular, they are, for the present purpose, governed by the same termination rate constant, k_t. Additional radical deactivation processes are indicated by

$$R_n + X \xrightarrow{k_m} P_n \tag{20}$$

The photopolymerization of monolayers prepared from mixtures of 1 and 5 (eq 16–20) is governed by the kinetic equations (eq 21–26).

$$d[M]/dt = \bar{\epsilon}\bar{I}\Phi_r[M] - k_p[M]\sum_{n=1}^{\infty}[R_n] \tag{21}$$

$$d[R_1]/dt = \bar{\epsilon}\bar{I}\Phi_r[M] - k_p[R_1][M] - k_m[R_1] - k_t[R_1]\sum_{n=1}^{\infty}[R_n] \tag{22}$$

$$\vdots$$

$$d[R_{i-1}]/dt = -k_p[R_i][M] + k_p[R_i][M] - k_m[R_{i-1}] - k_t[R_{i-1}]\sum_{n=1}^{\infty}[R_n] \tag{23}$$

$$d[R_i]/dt = -k_p[R_i][M] + k_p[R_{i-1}][M] - k_m[R_i] - k_t[R_i]\sum_{n=1}^{\infty}[R_n] \tag{24}$$

Summing the infinite number of equations in dR_i/dt, eq 25 and 26 describe the concentration changes of M and R during the photopolymerizations.

$$d[M]/dt = -\bar{\epsilon}\bar{I}\Phi_r[M] - k_p[M][R_n] \tag{25}$$

$$d[R]/dt = \bar{\epsilon}\bar{I}\Phi_r[M] - k_s[R] - k_t[R]^2, \text{ with } [R] \equiv \sum_{n=1}^{\infty}[R_n] \tag{26}$$

Assuming that photopolymerization of monolayers, similar to that of surfactant vesicles,[18] is a two-dimensional process, eq 25 and 26 can be linearized to

$$d[M]/dt = -\beta[M] + \gamma[R] \tag{27}$$

$$d[R]/dt = \beta[M] - \nu[R] \tag{28}$$

where

$$\gamma = -k_p w(t) \qquad \nu = k_m \tag{29}$$

$$\beta = \bar{\epsilon}\bar{I}\Phi_r \tag{30}$$

where $\bar{\epsilon}$ is the absorption cross section of the monolayer, $\bar{I}$ is the mean intensity of the light source, and Φ_r is the quantum efficiency for radical formation.[39]

With initial conditions such that $M(0) = M_0$ and $R(0) = 0$, the solution of eq 27 and 28 for [M] is

$$[M](t) = \frac{[M_0]}{\rho_2 - \rho_1}[(\rho_2 + \beta)e^{\rho_1 t} - (\rho_1 + \beta)e^{\rho_2 t}] \tag{31}$$

where

$$\rho_{1,2} = \tfrac{1}{2}[-(\beta + \nu) \pm [(\beta + \nu)^2 - 4\beta(\nu - \gamma)]^{1/2}] \tag{32}$$

With the simplification that $\rho_2 \gg \rho_1$ and $\rho_1 \gg \beta$, eq 31 yields

$$M(t) = M_0 e^{-t/\tau}; \quad \tau = -1/\rho_1 \tag{33}$$

which, by expressive changes of concentrations in terms of area changes, leads to eq 15.

The decay time (τ value) of the photopolymerization is related to

$$\tau = \frac{1}{\Phi_I \bar{I}\bar{\epsilon}} \frac{k_m + k_s}{k_m + k_p} \cong \frac{1}{\Phi_r \bar{I}\bar{\epsilon}} \frac{k_m + k_s}{k_p} \tag{34}$$

Since $k_p \gg k_m$, the average length of polymer chains, $\bar{L}$, can be approximated[18] by assuming it to be given by the ratio of average free radical propagation time to the average deactivation time per polymer link:

$$\bar{L} \simeq \frac{k_p}{k_m} \simeq \frac{1}{\Phi_i \bar{I} \bar{\epsilon} \tau} \quad (35)$$

The $\bar{L}$ values, assessed from eq 35 by using the obtained kinetic data, are also given in Table II.

The degree of photopolymerization of monolayers prepared from 1 is considerably greater than that observed for vesicles made from the same surfactant.[23] This fact has been rationalized in terms of tighter packing of the surfactants in monolayers than in vesicles. Paralleling the behavior of τ values, the degrees of photopolymerization are related to the intensity of irradiation and to the mole fraction of 1 in the mixture of 1 and 5. Decreasing the intensity of irradiation increased $\bar{L}$ values for monolayers prepared from 1[23] and from mixtures of 1 and 5. This trend persisted at two different surface pressures, 21 and 40 mN m^{-1} at $x_1 = 0.6$ (Table II).

The classical approach (CPM model) considers the apparent photoinitiation (v_i), propagation (v_p), and termination (v_t) rates:

$$v_i = k_0 \bar{I} \quad (36)$$

$$v_p = k_p[M][R^\bullet] \quad (37)$$

$$v_t = k_t[R^\bullet]^2 \quad (38)$$

where [M] and [R$^\bullet$] are the molecular area densities of the monomer and the propagating radical in the monolayer; k_0, k_p, and k_t are rate constants for photoinitiation, propagation, and termination, respectively; and $\bar{I}$ is the mean intensity of the light mediating the photopolymerization.[39]

Writing eq 36–38, we assumed that all the components of the light are absorbed for radical production so that v_i is independent of the monomer concentration. Under steady-state conditions

$$v_i = v_t \qquad [R] = [R]_s \quad (39)$$

$$k_0 \bar{I} = k_t[R]_s^2 \quad (40)$$

where $[R]_s$ is the molecular area density of the propagating radical under steady-state conditions. The apparent polymerization rate, V_R, is

$$V_R = v_i + v_p \quad (41)$$

and if the chains are long, $v_i \ll v_p$, eq 40 simplifies to

$$V_R = v_p = k_p[M](k_0/k_t)^{1/2} I^{1/2} \quad (42)$$

An advantage of the classical treatment of the kinetic data is that the average lifetime of the propagating radical, τ_{av}, can be assessed. The radical production rate is

$$d[R]/dt = k_0 \bar{I} - k_t[R]^2 \quad (43)$$

Substitution of eq 40 into eq 43 leads to

$$d[R]/dt = k_t([R]_s^2 - [R]^2) \quad (44)$$

which upon integration becomes

$$\ln\left(\frac{1 + [R]/[R]_s}{1 - [R]/[R]_s}\right) = 2k_t[R]_s t \quad (45)$$

The average chain radical lifetime, τ_{av}, is defined as

$$\tau_{av} = \frac{[R]_s}{k_t[R]_s^2} = \frac{1}{k_t[R^\bullet]_s} \quad (46)$$

and the change of monomer concentration with time, expressed in terms of surface area changes, $\Delta(n)$, is given by

$$\Delta[n] = \int_{t_t}^{t_s} k_p[M][R]\, dt \quad (47)$$

where t_t and t_s represent some initial irradiation time and the time when the steady state of polymerization has been reached. Integration of eq 47 yields

$$\Delta(n) = k_p[M][R]\tau_{av} \ln \cosh (t/\tau_{av}) \quad (48)$$

which upon rearrangement ($t \gg \tau_{av}$) results in

$$\frac{\Delta[n]}{[n]} = \frac{k_p}{k_t}\frac{1}{\tau_{av}} t - \frac{k_p}{k_t} \ln 2 \quad (49)$$

Thus, a plot of the left-hand side of eq 49 against time (t) should give straight lines from which the slopes and intercepts τ_{av} and k_p/k_t can be calculated. Plots of the data according to eq 49 are given in Figure 6 and τ_{av} and k_p/k_t values are collected in Table II.

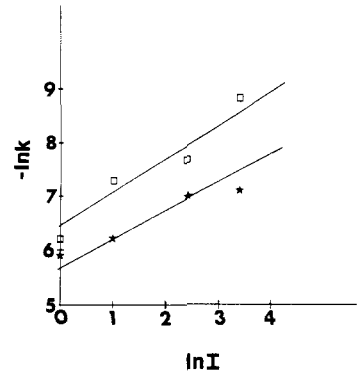

Figure 7. Plots of the logarithms of polymerization rates against the logarithm of intensities of polymerizations of monolayers prepared from 1 + 5 ($x_1 = 0.6$) at $\Pi = 40$ mN m^{-1} (□) and $\Pi = 21$ mN m^{-1} (★). k is defined as the first-order rate constant.

Both the PPM (eq 15 and 34) and the CPM (eq 42) models predict a first-order change of the monomer surface area as a function of the irradiation time. The two models predict, however, different intensity relationships. Plots of the logarithms of photopolymerization rates (log V_r in eq 42 and log $1/\tau$ in eq 34) against the logarithms of light intensities ($\bar{L}$) should give straight lines with a slope of 0.5 if eq 42 prevails and a slope of 1 if eq 34 represents a better model. Figure 7 shows such plots for the photopolymerization of monolayers prepared from a $x_1 = 0.6$ mixture of 1 and 5 at $\Pi = 21$ and $\Pi = 40$. The slopes of these plots, 0.58 and 0.63, respectively, indicate that the classical photopolymerization model satisfactorily describes the results. It is interesting to note that slopes of similar plots obtained in the photopolymerization of monolayers prepared from 1 (i.e., $x_1 = 1.0$) had values that depended on the level of irradiation. Slopes of 0.95 and 0.40 were obtained for photopolymerizations mediated by high (laser) and low (steady-state) intensity irradiations.[23]

Acknowledgment. Support of this work by the National Science Foundation is gratefully acknowledged.

Registry No. 1, 96478-22-7; 5, 3700-67-2.

References and Notes

(1) Permanent address: Department of Modern Chemistry, University of Science and Technology of China, Hefei, China.
(2) Swalen, J. D.; Allara, D. L.; Andrade, J. D.; Chandross, E. A.; Garoff, S.; Israelachvili, J.; McCarthy, T. J.; Murray, R.; Pease, R. F.; Rabolt, J. F.; Wynne, K. J.; Yu, H. *Langmuir* **1987**, *3*, 932–950.
(3) Roberts, G. G. *Adv. Phys.* **1985**, *34*, 475–512.
(4) Carter, F. L. *Molecular Electronic Devices*; Marcel Dekker: New York, 1987.
(5) The number of papers presented at the International Conferences on Langmuir–Blodgett Films increased from 49 in 1982 (see: *Thin Solid Films* **1983**, *99*, 1–329) to 79 in 1985 (see: *Thin Solid Films* **1985**, *132*, *133*, *134*, 1–736).
(6) Fendler, J. H. In *Surfactants in Solution*; Mittal, K. L., Lindman, B., Eds.; Plenum Press: New York, 1984; pp 1947–1989.

(7) Dubault, A.; Casagrande, C.; Veyssie, M. *J. Phys. Chem.* **1975**, *79*, 2254-2259.
(8) Letts, S. A.; Fort Jr., T.; Lando, J. B. *J. Colloid Interface Sci.* **1976**, *56*, 64-75.
(9) Day, D. R.; Ringsdorf, H. *Makromol. Chem.* **1979**, *180*, 1059-1063.
(10) O'Brien, K. C.; Rogers, C. E.; Lando, J. B. *Thin Solid Films* **1983**, *102*, 131-140.
(11) Hupfer, B.; Ringsdorf, H. *Chem. Phys. Lipids* **1983**, *33*, 263-282.
(12) Holden, D. A.; Ringsdorf, H.; Haubs, M. *J. Am. Chem. Soc.* **1984**, *106*, 4531-4536.
(13) Elbert, R.; Laschewsky, A.; Ringsdorf, H. *J. Am. Chem. Soc.* **1985**, *107*, 4134-4141.
(14) Higashi, N.; Kunitake, T. *Chem. Lett.* (*Jpn.*) **1986**, *105*-108.
(15) Laschewsky, A.; Ringsdorf, H.; Schmidt, G.; Schneider, J. *J. Am. Chem. Soc.* **1987**, *109*, 788-796.
(16) Fendler, J. H.; Tundo, P. *Acc. Chem. Res.* **1984**, *17*, 3-7.
(17) Rolandi, R.; Flom, S. R.; Dillon, I.; Fendler, J. H. *Prog. Colloid Polym. Sci.* **1987**, *73*, 134-141. Zhao, X. K.; Baral, S.; Rolandi, R.; Fendler, J. H. *J. Am. Chem. Soc.* **1988**, *110*, 1012-1024.
(18) Reed, W.; Guterman, L.; Tundo, P.; Fendler, J. H. *J. Am. Chem. Soc.* **1984**, *106*, 1897-1907.
(19) Nome, F.; Reed, W.; Politi, M.; Tundo, P.; Fendler, J. H. *J. Am. Chem. Soc.* **1984**, *106*, 8086-8093.
(20) Serrano, J.; Mucino, S.; Millan, S.; Reynoso, R.; Fucugauchi, L. A.; Reed, W.; Nome, F.; Tundo, P.; Fendler, J. H. *Macromolecules* **1985**, *18*, 1999-2005.
(21) Reed, W.; Lasic, D.; Hauser, H.; Fendler, J. H. *Macromolecules* **1985**, *18*, 2005-2012.
(22) Yuan, Y.; Tundo, P.; Fendler, J. H. *Macromolecules* **1989**, *22*, 29-35.
(23) Rolandi, R.; Paradiso, R.; Xu, S. Q.; Palmer, C.; Fendler, J. H. *J. Am. Chem. Soc.*, in press.
(24) Mingins, J.; Owens, N. F. *Thin Solid Films* **1987**, *152*, 9-28.
(25) Gaines, G. L., Jr. *J. Colloid Interface Sci.* **1966**, *21*, 315-319.
(26) Goodrich, F. C. *Proc. 2nd Int. Congr. Surf. Activity I* **1951**, 85-91.
(27) Gaines, G. L. *Insoluble Monolayers at Liquid-Gas Interfaces*; Wiley: New York, 1966.
(28) Gershfeld, N. L. *Ann. Rev. Phys. Chem.* **1976**, *27*, 349-368.
(29) Joos, P. *Bull. Soc. Chim. Belges* **1969**, *78*, 207-217.
(30) Joos, P.; Demel, R. A. *Biochim. Biophys. Acta* **1969**, *183*, 447-457.
(31) Zsako, J.; Tomoaia-Cotisel, M.; Chifu, E. *J. Colloid Interface Sci.* **1984**, *102*, 186-205.
(32) Defay, R.; Prigogine, I.; Bellemans, A.; Evertt, D. H. *Surface Tension and Adsorption*; Longmans & Green: London, 1966.
(33) Costin, I. S.; Barnes, G. T. *J. Colloid Interface Sci.* **1975**, *51*, 106-121.
(34) Tancrède, P.; Parent, L.; Leblanc, R. M. *J. Colloid Interface Sci.* **1982**, *89*, 117-123.
(35) Robert, S.; Tancrède, P.; Salesse, C.; Leblanc, R. M. *Biochim. Biophys. Acta* **1983**, *730*, 217-225.
(36) Tancrède, P.; Munger, G.; Leblanc, R. M. *Biochim. Biophys. Acta* **1982**, *689*, 45-54.
(37) Thin-layer chromatography of polymerized vesicles prepared from 1 showed no traces of cleaved products. Presence of 1% deliberately added single-chain carboxylic acid surfactant was shown to be detectable.
(38) Flory, P. J. *Principles of Polymer Chemistry*; Cornell University Press: Ithaca, N.Y. 1953; p 111.
(39) The value of Φ_r has been determined to be 0.106.[17] The molar extinction coefficient ($\epsilon_{266\ nm}$ = 1600 M^{-1} cm^{-1}) was converted to a molecular cross section by $\epsilon_{266\ nm} = 1.6 \times 10^3$ M^{-1} cm^{-1} $L(10^3\ cm^3)/L \times 1$ mol/$(6.02 \times 10^{23}$ monomer) = 2.7×10^{-18} cm^2/monomer. Table II gives $\bar{\epsilon I}$ values ($\bar{\epsilon I}$ = integral ($\lambda_1 \rightarrow \lambda_2$) of $\bar{\epsilon I}$ dλ) values for steady-state irradiation intensities. Using a very narrow band path ($^1/_2$ half-bandwidth = 5 nm) allowed us to carry out the integration between 243 and 250 nm.

Temperature Dependence of Crystal Lattice Modulus and Dynamic Mechanical Properties of Ultradrawn Polypropylene Films

Chie Sawatari† and Masaru Matsuo*

Department of Clothing Science, Faculty of Home Economics, Nara Women's University, Nara 630, Japan. *Received May 5, 1988; Revised Manuscript Received November 29, 1988*

ABSTRACT: The temperature dependence of the crystal lattice modulus of polypropylene was measured by X-ray diffraction using ultradrawn films produced by gelation/crystallization from solutions. Measurements were carried out in the temperature range 20–160 °C for specimens with draw ratios of about 100. The measured crystal lattice modulus was in the range 40.6–41.4 GPa, and the values were independent of temperature. In contrast, the storage modulus of the films decreased with increasing temperature. This discrepancy was related to an increase in the amorphous content with increasing temperature, and this tendency became enhanced at temperatures above 130 °C. Furthermore, in terms of relative molecular orientation, the relaxation mechanism was discussed as a function of draw ratio by using master curves constructed by shifting horizontally and then vertically. Thus the Arrhenius plots of log shift factor versus reciprocal of the absolute temperature indicate that there exist two mechanical dispersions corresponding to the α and β mechanisms for drawn specimens with draw ratios >100. The values of activation energies associated with the α and β mechanisms decrease accordingly as the draw ratio increases. Incidentally, the values, 129 and 82 kJ/mol, of the α and β mechanisms for the undrawn films are lower than those reported already.

Introduction

It is well-known that molecular chains with ultradrawn films are aligned almost perfectly in the stretching direction. Such a simple morphology has the advantage of permitting an estimate of the crystal lattice modulus and the mechanical dispersion of polymeric materials.[1,2] On the basis of this concept, Matsuo et al. have studied the temperature dependence of the crystal lattice modulus[3] and the crystal dispersion[4,5] using ultradrawn polyethylene films prepared by gelation/crystallization from dilute solution by the method of Smith and Lemstra[6,7] and then were elongated in a hot oven at 135 °C. The temperature dependence of the crystal lattice modulus was measured in the temperature range 20–150 °C for the specimens with the draw ratios >300.[3] The resultant values were independent of temperature up to 145 °C (close to the theoretical melting point of 145.5 °C[8]) and were in the range 211–222 GPa. In contrast, although the storage modulus

* To whom correspondence should be addressed.
† Present address: Faculty of Education, Shizuoka University, Shizuoka 442, Japan.

0024-9297/89/2222-2968$01.50/0